

Symmetry-dependent vibrational excitation in N 1s photoionization of N₂: Experiment and theory

M. Ehara^{a),b)}

Department of Synthetic Chemistry and Biological Chemistry, Graduate School of Engineering, Kyoto University, Kyoto 615-8510, Japan

H. Nakatsuji^{a),c)}

Department of Synthetic Chemistry and Biological Chemistry, Graduate School of Engineering, Kyoto University, Kyoto 615-8510, Japan and Fukui Institute for Fundamental Chemistry, Kyoto University, Kyoto 606-8103, Japan

M. Matsumoto, T. Hatamoto, X.-J. Liu, T. Lischke, and G. Prümper

Institute of Multidisciplinary Research for Advanced Materials, Tohoku University, Sendai 980-8577, Japan

T. Tanaka, C. Makochekanwa, M. Hoshino, and H. Tanaka

Department of Physics, Sophia University, Tokyo 102-8854, Japan

J. R. Harries and Y. Tamenori

Spring-8/JASRI, Sayo-gun, Hyogo 679-5198, Japan

K. Ueda^{a),d)}

Institute of Multidisciplinary Research for Advanced Materials, Tohoku University, Sendai 980-8577, Japan

(Received 19 December 2005; accepted 6 February 2006; published online 27 March 2006)

We have measured the vibrational structures of the N 1s photoelectron mainline and satellites of the gaseous N₂ molecule with the resolution better than 75 meV. The gerade and ungerade symmetries of the core-ionized (mainline) states are resolved energetically, and symmetry-dependent angular distributions for the satellite emission allow us to resolve the Σ and Π symmetries of the shake-up (satellite) states. Symmetry-adapted cluster-expansion configuration-interaction calculations of the potential energy curves for the mainline and satellite states along with a Franck-Condon analysis well reproduce the observed vibrational excitation of the bands, illustrating that the theoretical calculations well predict the symmetry-dependent geometry relaxation effects. The energies of both mainline states and satellite states, as well as the splitting between the mainline gerade and ungerade states, are also well reproduced by the calculation: the splitting between the satellite gerade and ungerade states is calculated to be smaller than the experimental detection limit. © 2006 American Institute of Physics. [DOI: 10.1063/1.2181144]

I. INTRODUCTION

Electronically excited states often have individual stable geometries that are different from the ground state and thus photoexcitation causes a sudden redistribution of electric charge. The nuclei cannot adapt to this on the same time scale and are considered stationary during an electronic transition—the well-known Franck-Condon (FC) principle. In consequence, the final state is often left vibrationally excited. One can obtain information on the stable geometry of the electronically excited state by analyzing the vibrational population distribution of the excited state on the basis of the FC principle.¹

The high photon flux at very narrow photon bandwidths available using high-resolution soft x-ray monochromators installed at high-brilliance third-generation synchrotron radiation light sources has stimulated a renewal of interest in

core-level photoelectron spectroscopy.²⁻⁵ One can observe vibrational structures in the core-level photoelectron mainline spectrum and thereby discuss the stable geometry of the single-hole (mainline) states. Previously, we have investigated vibrationally resolved C and O 1s photoelectron spectra of CO both experimentally and theoretically:⁶ potential curves for the C 1s and O 1s single-hole states were extracted from experimentally determined vibrational intensity ratios on the basis of a FC analysis and were well reproduced by *ab initio* calculations based on the symmetry-adapted cluster-expansion configuration-interaction (SAC-CI) method.⁷⁻¹⁰ Furthermore, we observed vibrationally resolved photoelectron satellite bands arising from C 1s photoionization¹¹ in CO, in which two-hole one-electron (satellite) states of Σ and Π symmetries were resolved using an angle-resolved technique. *Ab initio* calculations based on the SAC-CI method well reproduced the vibrational excitation of the observed satellite bands.¹¹

In the present work, we extend our investigations to vibrational excitation in N 1s photoionization of N₂. Compared to CO, N₂ has one additional complication: each of the main-

^{a)}Authors to whom correspondence should be addressed.

^{b)}Electronic mail: ehara@sbchem.kyoto-u.ac.jp

^{c)}Electronic mail: hiroshi@sbchem.kyoto-u.ac.jp

^{d)}Electronic mail: ueda@tagen.tohoku.ac.jp

line and satellite states splits into closely separated gerade and ungerade states. The energy separation between the mainline gerade and ungerade states is only 100 meV but still one can experimentally separate these states. Hergenbahn *et al.* noted that different FC factors were needed for the two different states.¹² Recent *ab initio* calculations by means of the fourth-order Green's function method, referred to as ADC(4), indeed revealed that the stable geometries are different for the gerade and ungerade mainline states.¹³ It should also be noted that experimental and theoretical evidences for differences in the carbon-carbon bond length for the *u* and *g* core-hole states have been reported for acetylene,⁴ which is isoelectronic with N₂. Further experimental and theoretical investigations will be helpful to confirm quantitatively the difference of the stable geometries for the *u* and *g* core-hole states of N₂. As for the satellite states, Angonoa *et al.* calculated vertical spectra in N 1*s* photoionization of N₂ using the ADC(4) method.¹⁴ According to their calculations, in the region of 8–10 eV relative to mainline, the bands arising from the transitions of the two Π satellite states may be overlapped with those of the Σ satellite states. The *K*-shell satellite spectra of N₂ have also been studied experimentally.^{15–17} In particular, Kempgens *et al.* gave the assignments for the decomposed low-lying satellite bands: the vibrational structure was, however, not identified.¹⁷ Thus, there has been no investigation on the potential curves of these satellite states or vibrational excitation in these satellite states.

In the present experiment we have recorded photoelectron spectra of the N 1*s* mainline and low-lying satellite bands. High resolution (<75 meV) has allowed us to resolve the energy separation of the single-hole gerade and ungerade states as well as the vibrational structures of the single-hole and two-hole one-electron states. The observed satellite bands include one Σ state and two Π states that are energetically overlapped. These three bands are separated in the angle-resolved spectra, due to the symmetry-dependent angular anisotropy of the satellite photoemission. The observed individual vibrational structures for these bands provide key information about the potential curves of the states. A FC analysis based on *ab initio* potential curves calculated by means of the SAC-CI method well reproduces the vibrational structures for both the mainline and satellite bands: the SAC-CI method has been shown to be accurate for the various kinds of inner-shell electronic processes.^{11,18–21}

II. EXPERIMENT

The experiment was carried out at the high-resolution soft x-ray photochemistry beam line 27SU (Refs. 22 and 23) at SPring-8, Japan. The light source of the beam line is a figure-8 undulator,²⁴ which produces horizontal linearly polarized light from its first-order harmonic and vertical

linearly polarized light from the so-called 0.5th order harmonic. The electron spectroscopy apparatus has been described elsewhere²⁵ and only some specific features are summarized here. The apparatus consists of an electron energy analyzer (Gammadata-Scienta SES-2002), a gas cell, and a differentially pumped main chamber. The lens axis of the analyzer is set in a horizontal direction so that the entrance slit of the analyzer is parallel to the incident photon beam. The whole system sits on an adjustable stage so that the source point of the analyzer can be adjusted easily relative to the fixed beam position. For angle-resolved electron spectroscopy, the spectrometer is fixed in this state, and the direction of the electric vector of the incident beam is switched between the horizontal and vertical directions. The degree of linear polarization was measured by observing the Ne 2*s* and 2*p* photolines and found to be greater than 0.98 for the current optical settings, enabling the assumption that all photons are completely polarized.

III. COMPUTATION

As was noted by Bagus and Schaeffer²⁶ over 30 years ago and elaborated by Sawatzky and Lenseling,²⁷ core ionization in symmetric molecules presents some special challenges for theory. We expect these systems to be described by wave functions that are adapted for the symmetry of the molecule, *u* and *g* in the present N₂ case. However, at the Hartree-Fock (HF) level calculations, such wave functions give ionization energies that are too high. At this level of calculations, correct ionization energies are obtained only by localizing the core hole on one side of the equivalent atoms. The implication is that there is a very large amount of core-valence correlation. This effect can be included only by using a large basis set and CI properly. Keeping these points in mind, we have carried out the extensive *ab initio* calculations for the potential energy curves of the ground and N 1*s* single-hole states, ²Σ⁺, ²Π, ²Δ, and ²Σ⁻ satellite states for both gerade and ungerade symmetries in the region of *R*=0.9–1.8 Å. Extensive basis sets were used to allow the description of the orbital reorganization and electron correlations; triple zeta (10*s*6*p*)/[5*s*3*p*] of Schaefer *et al.*²⁸ with two polarization *d* functions.²⁹ In the SAC-CI calculation, single to quadruple *R* operators^{9,30–32} were included to describe the electron correlations and orbital relaxation; these higher-order operators are necessary for describing orbital relaxations as well as electron correlations. For reference orbitals, ground-state HF with canonical molecular orbitals (MOs) were used; core-localized orbital was not adopted. All MOs were included in the active space to describe core-hole relaxation. In the calculation of 1σ_{*u*} single-hole and ungerade shake-up satellite states, *R* operators with a hole of 1σ_{*u*} and 1σ_{*g*} orbitals were generated. This approach is relevant to get a precise N 1*s* ionization potential. This is also approach for the gerade states. To reduce the computational requirements, the perturbation selection procedure³³ was adopted. The threshold of the linked terms for the ground state was set to 1.0 × 10⁻⁶ a.u., and the unlinked terms were adopted as products of the important linked terms with singles and doubles

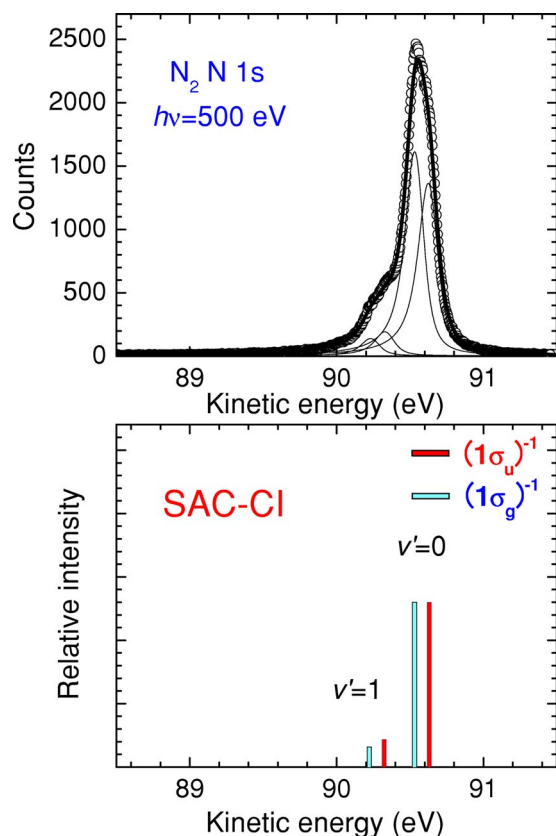


FIG. 1. Vibrationally resolved photoelectron spectra of the $1\sigma_g$ and $1\sigma_u$ ionized states of N₂. Upper panel: circle, experiment; thick line, fitted modeled spectrum; thin lines, individual peaks. Lower panel: SAC-CI spectrum.

configuration interaction (SDCI) coefficients greater than 0.005. For the inner-shell shake-up satellite states, all the single and double operators were included without selection, and the thresholds of the higher triples and quadruples were set to 1.0×10^{-7} a.u. The reference functions of the perturbation selection were chosen from the singles, doubles, and triples (SDT)-CI solutions. The thresholds of the CI coefficients for calculating the unlinked operators in the SAC-CI method were 0.05 and 0.0 for the R and S operators, respectively. The calculated potential energy curves were fitted with fifth-order extended Rydberg functions and vibrational analysis was performed. For simulating the photoelectron spectrum, vibrational wave functions and FC factors were obtained using the grid method in which the Lanczos algorithm was adapted for the diagonalization. The SAC/SAC-CI calculations were executed with the GAUSSIAN 03 suite of programs³⁴ with some modifications for calculating inner-shell ionization spectra; namely, reference SDT-CI with both $1\sigma_u$ and $1\sigma_g$ core-hole configurations was enabled in the SAC-CI calculation. The N 1s adiabatic ionization potentials thus calculated are 410.14 and 410.24 eV for $1\sigma_u$ and $1\sigma_g$ ionized states, respectively. These values are in reasonable agreement with the experimental values,³⁵ 409.82 and 409.93 eV, respectively, and confirm that the large amount of core-valence correlation is indeed properly taken into account in the present calculations. The vibrational analysis was performed with the MCTDH program package.³⁶

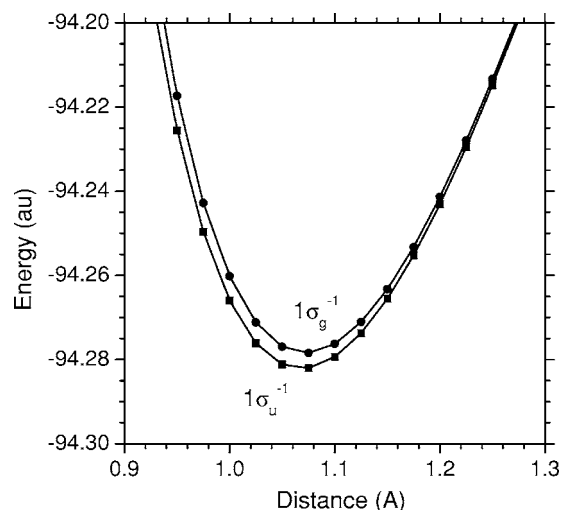


FIG. 2. Calculated potential energy curves of the $1\sigma_g$ and $1\sigma_u$ ionized states of N₂.

IV. RESULTS AND DISCUSSION

A. Vibrationally resolved spectra of main lines

The ground state of the N₂ molecule has the electron configuration

$$(1\sigma_g)^2(1\sigma_u)^2(2\sigma_g)^2(2\sigma_u)^2(1\pi_g)^4(3\sigma_g)^2; {}^1\Sigma_g^+.$$

Two almost degenerate core orbitals $1\sigma_g$ and $1\sigma_u$ are associated with the symmetric and antisymmetric linear combinations of the atomic 1s orbitals, respectively. Photoionization of N 1s mostly leads to nearly degenerate single-hole states and with a certain probability to two-hole one-electron states. The single-hole states have g and u symmetries corresponding to the creation of a single-hole in $1\sigma_g$ and $1\sigma_u$, respectively. In this subsection, we discuss the main line of the N 1s photoelectron spectra of N₂.

Figure 1 compares the N 1s photoelectron spectrum recorded at a photon energy 500 eV to the calculated SAC-CI spectra. The experimental spectrum has been decomposed by least-squares curve fitting into a vibrational progression. In this fit a post-collision interaction (PCI)-distorted line profile is convoluted with a Gaussian profile. The positions of the individual vibrational components and their intensities were treated as fitting parameters.

About ten N 1s photoelectron spectra were recorded over a photon energy range of 440–550 eV and decomposed into vibrational components by curve fitting. The Gaussian widths representing a convolution of the monochromator bandwidth, electron analyzer bandwidth, and Doppler broadening are 75 meV or less depending on the kinetic energy. In the fitting, the Lorentzian widths were fixed to the values previously determined: 116 meV for $1\sigma_g^{-1}$ and 124 meV for $1\sigma_u^{-1}$. The intensity ratios of the $v'=1$ peak to the main $v'=0$ peak, $I(v'=1)/I(v'=0)$, are almost constant over the kinetic energy region of 50–140 eV. From this analysis, we extract the intensity ratio at the sudden limit. The FC ratio $I(v'=1)/I(v'=0)$ for the gerade and ungerade states were thus estimated to be 0.079(5) and 0.146(8), respectively.

Figure 2 shows the calculated potential energy curves of the $1\sigma_u$ and $1\sigma_g$ ionized states. Based on these curves, a

TABLE I. Spectroscopic constants of the ground and N 1s ionized states, $1\sigma_g$ and $1\sigma_u$ of N_2 . ΔR_e is the difference of the bond lengths between the neutral and ionic species. $I(v'=1)/I(v'=0)$ is the intensity ratio.

State	Present work		
	Experiment	SAC-CI	CCSD(T)+ADC(4) ^a
Ground			
R_e (Å)	1.0977	1.095	1.093
ω_e (cm ⁻¹)	2359	2416	2372
$\omega_e\chi_e$ (cm ⁻¹)	14.3	13.8	14.6
N 1 σ_u ionized			
$I(v'=1)/I(v'=0)$	0.146 (8)	0.168	0.115
R_e (Å)	1.0743(8)	1.068	1.072
ΔR_e (Å)	-0.0234(8)	-0.027	-0.021
ω_e (cm ⁻¹)	2403(28)	2492	2437
$\omega_e\chi_e$ (cm ⁻¹)	...	5.6	17.8
N 1 σ_g ionized			
$I(v'=1)/I(v'=0)$	0.079(5)	0.122	0.081
R_e (Å)	1.0798(7)	1.072	1.076
ΔR_e (Å)	-0.0179(7)	-0.023	-0.017
ω_e (cm ⁻¹)	2417(23)	2486	2440
$\omega_e\chi_e$ (cm ⁻¹)	...	4.2	18.3

^aReference 13.

vibrational analysis was performed, and the obtained spectroscopic constants are summarized in Table I along with the experimental values. Table I also includes the relevant theoretical values for the $1\sigma_u$ and $1\sigma_g$ ionized states calculated by Thiel *et al.*¹³ using the CCSD(T)+ADC(4) technique. The spectroscopic constants of the ground state were calculated to be $\omega_e=2416$ cm⁻¹ and $\omega_e\chi_e=13.8$ cm⁻¹, in comparison with the experimentally derived values of $\omega_e=2359$ cm⁻¹ and $\omega_e\chi_e=14.3$ cm⁻¹.¹ The deviations from the experimental values are due to the neglect of triple and higher operators; the CCSD(T) calculation with the same level of basis sets gave $\omega_e=2372$ cm⁻¹ and $\omega_e\chi_e=14.6$ cm⁻¹.¹³ In the $1\sigma_u$ and $1\sigma_g$ ionized states, the bond length was predicted to shrink by 0.027 and 0.023 Å, respectively, in good agreement with the experimental estimates of $\Delta R_e=-0.023$ and -0.018 Å. The geometry relaxation of the $1\sigma_u$ state is larger than that of the $1\sigma_g$ state, since the $1\sigma_u$ state is accessed by ionization from an antiphase orbital. The vibrational frequencies of these states were calculated to be $\omega_e=2492$ and 2486 cm⁻¹ for $1\sigma_u$ and $1\sigma_g$, larger than the experimental values of $\omega_e=2403$ and 2417 cm⁻¹, determined by adopting the harmonic approximation. For these values, the CCSD(T)+ADC(4) method gave good results.¹³

The Franck-Condon factors (FC factors) between the ground and core-ionized states were also calculated from the vibrational wave functions. The SAC-CI $I(v'=1)/I(v'=0)$ ratios were 0.168 and 0.122 for the $1\sigma_u$ and $1\sigma_g$ states, in reasonable agreement with the experimental values of 0.146(8) and 0.079(5). The agreement for the C 1s ionized state of CO¹¹ was more encouraging than for the present N_2 case; this suggests that the description of the orbital relaxation of the N 1s ionization is still less accurate than for the

C 1s ionization, due to the difficulty of dealing with the correlational effects intrinsic to the homonuclear diatomic molecules described in the previous section.

B. Vibrationally resolved spectra of the satellite bands

Photoelectron satellites provide evidence for the breakdown of the independent particle picture and are thus called correlation satellites.^{37,38} The correlation satellites can be classified into two groups phenomenologically.³⁹ The first group includes satellites whose excitation cross sections relative to the single-hole ionization cross section stay relatively constant, while the second group includes those whose excitation cross sections sharply decrease with an increase in energy. These two different types of energy dependence have been attributed to the two lowest-order correlation terms, often called the direct and conjugate shake-up terms.⁴⁰ The conjugate shake-up contribution is significant near the ionization threshold region and decreases rapidly with increasing energy.^{38,40} The conjugate contributions become negligible at high energy because of the sharp drop of the bound-free overlap integral. At this limit, the direct shake-up satellite band mimics the mainline both in the excitation cross section and in the asymmetry parameter β of the electron emission: β approaches the limiting value two. It should be noted that the direct and conjugate channels may have the same final state and thus interference may take place.⁴¹

The low-lying two-hole one-electron states concerned here have electron configurations $1\sigma_u^{-1}1\pi_u^{-1}1\pi_g^1(2\Sigma_g^+)$, $1\sigma_u^{-1}1\pi_u^{-1}1\pi_g^1(2\Sigma_u^+)$, $1\sigma_g^{-1}3\sigma_g^{-1}1\pi_g^1(2\Pi_g)$, and $1\sigma_u^{-1}3\sigma_g^{-1}1\pi_g^1(2\Pi_u)$. The transitions leading to the $1\sigma_u^{-1}1\pi_u^{-1}1\pi_g^1(2\Sigma_g^+)$ and $1\sigma_g^{-1}1\pi_u^{-1}1\pi_g^1(2\Sigma_u^+)$ states are dominated by the direct shake-up term: the conjugate shake-up term also contributes at low excitation energy. The transitions leading to $1\sigma_g^{-1}3\sigma_g^{-1}1\pi_g^1(2\Pi_g)$ and $1\sigma_u^{-1}3\sigma_g^{-1}1\pi_g^1(2\Pi_u)$ states are dominated by the conjugate shake-up contribution. According to Angonoa *et al.*,¹⁴ the vertical ionization energy of the $2\Sigma_g^+$ state was estimated to be 9.32 eV while those of $2\Pi_g$ were 8.46 and 10.01 eV. Thus the low-lying photoelectron satellite bands arising from the transitions to the $2\Sigma_g^+$ and $2\Pi_{g,u}$ states are expected to overlap in energy.

Figure 3 shows the low-lying satellite bands recorded at photon energies of 427.5, 430, 435, and 450 eV at 0° and 90° relative to the polarization vector of the incident radiation. In the 90° spectrum at 427.5 eV, we can see two vibrational bands. Looking at the 0° spectrum, we notice that there are some peaks which are not seen in the 90° spectrum. When the photon energy is increased from 427.5 to 450 eV, we see a dramatic change in the spectra. This change is due to a rapid intensity drop of the 90° spectrum and of the same band in the 0° spectrum. From these spectra, it is clear that there are at least three electronic states involved.

Based on the observed energy dependence and angular distribution of the satellite spectra, we can decompose the contributions from the direct and conjugate terms as discussed in detail in our previous paper.¹¹ Using the characteristics of the direct and conjugate shake-up contributions described above, we can assign the observed three vibrational

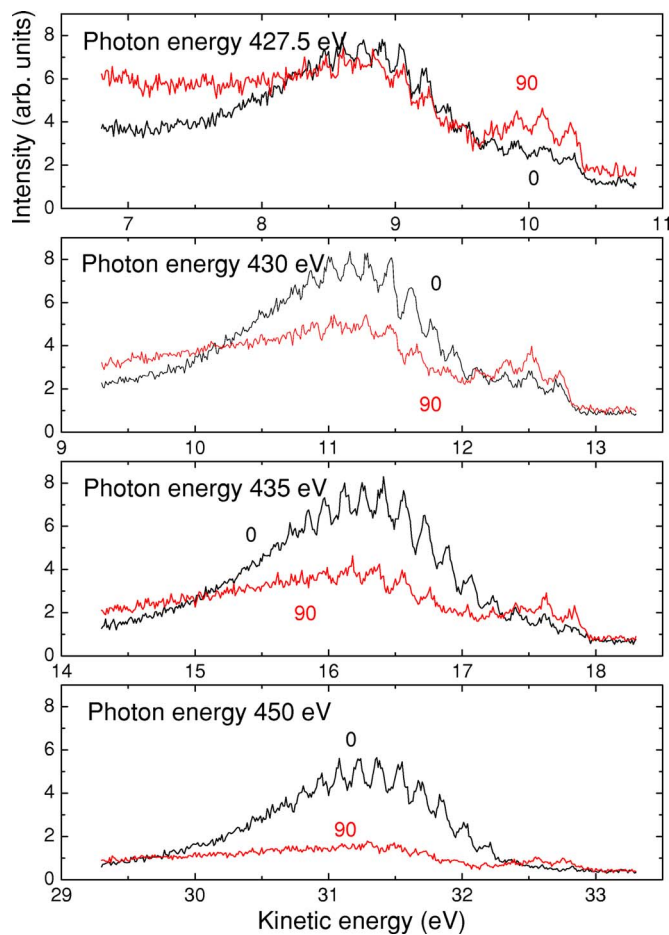


FIG. 3. N 1s photoelectron satellite spectra of N₂ recorded at photon energies of 427.5, 430, 435, and 450 eV, at 0° (black lines) and 90° (red lines) to the polarization vector (of the incident radiation) plotted as a function of photoelectron kinetic energy.

bands in Fig. 3. The band which appears in the 0° spectrum at 450 eV nearly disappears in the 90° spectrum, exhibiting a very strong anisotropy with β close to two. Thus we can conclude that this band is dominated by the direct shake-up contribution and assign it to transition to the ionic final states $1\sigma_u^{-1}1\pi_u^{-1}1\pi_g^1(2\Sigma_g^+)$ and $1\sigma_g^{-1}1\pi_u^{-1}1\pi_g^1(2\Sigma_u^+)$. On the other hand, the two bands which appear in the 90° spectrum at 450 eV can be attributed to the conjugate shake-up contributions and thus are assigned to the transitions to the $1\sigma_g^{-1}3\sigma_g^{-1}1\pi_g^1(2\Pi_g)$ and $1\sigma_u^{-1}3\sigma_g^{-1}1\pi_g^1(2\Pi_u)$ states. The vibrational structure observed in each band includes information

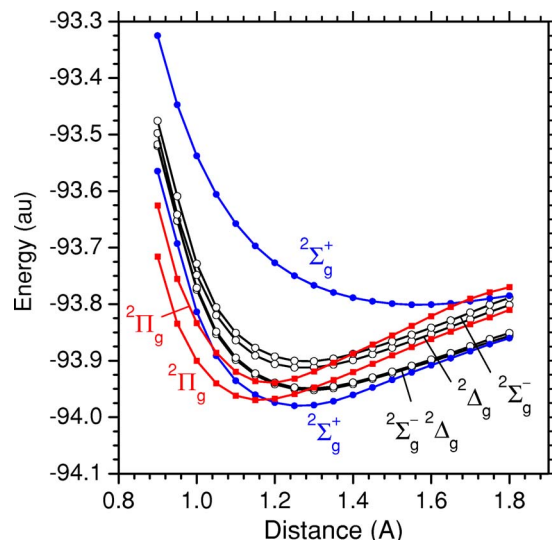


FIG. 4. Calculated potential energy curves of the N 1s shake-up satellite $2\Sigma_g^+$, $2\Pi_g$, $2\Sigma_g^-$, and Δ_g states of N₂.

on the potential curves of the relevant satellite state. However, the contribution from the Σ band to the 90° spectrum and the Π bands to the 0° spectrum may be non-negligible, and the β for the individual vibrational components are not necessarily the same.

We have performed *ab initio* calculations of the relevant potential curves by means of the SAC-CI method. The resulting potential energy curves of the N 1s two-hole one-electron satellite states of gerade symmetry are shown in Fig. 4. The potential curves of the counterpart ungerade states almost overlap with the corresponding gerade states. The overall characters of the potential energy curves are similar to those of CO,¹¹ which is isoelectronic with N₂. The spectroscopic constants of these satellite states were summarized in Table II. The geometry relaxation by shake-up ionization of N₂ is large for the $2\Sigma_g^+$ state, and the calculated value of r_e is 1.259 Å, 0.164 Å longer than that of the ground state. This change is almost the same to that in CO, since the shake-up states are characterized by $\pi-\pi^*$ transitions for both molecules. For the ungerade state $2\Sigma_u^+$, the present calculation gives similar spectroscopic constants to $2\Sigma_g^+$: the equilibrium distances of $2\Sigma_{g,u}^+$ states are almost the same. Since the gerade state $2\Sigma_g^+$ has a hole in the $1\sigma_u$ orbital, it is located slightly lower in energy than the ungerade state $2\Sigma_u^+$. The

TABLE II. Spectroscopic constants of the low-lying N 1s satellite states calculated with the SAC-CI method.

Gerade states				Ungerade states			
State	R_e (Å)	ω_e (cm ⁻¹)	$\omega_e\chi_e$ (cm ⁻¹)	State	R_e (Å)	ω_e (cm ⁻¹)	$\omega_e\chi_e$ (cm ⁻¹)
$2\Pi_g$ (lower)	1.161	1868	21	$2\Pi_u$ (lower)	1.157	1787	13
$2\Pi_g$ (higher)	1.186	2090	27	$2\Pi_u$ (higher)	1.183	2049	28
$2\Sigma_g^+$ (lower)	1.259	1608	6	$2\Sigma_u^+$ (lower)	1.260	1609	8
$2\Delta_g$ (lower)	1.288	1420	7	$2\Delta_u$ (lower)	1.288	1459	10
$2\Sigma_g^-$ (lower)	1.288	1417	7	$2\Sigma_u^-$ (lower)	1.286	1471	12
$2\Delta_g$ (higher)	1.271	1508	10	$2\Delta_u$ (higher)	1.271	1581	16
$2\Sigma_g^-$ (higher)	1.277	1417	7	$2\Sigma_u^-$ (higher)	1.277	1527	10
$2\Sigma_g^+$ (higher)	1.568	905	5	$2\Sigma_u^+$ (higher)	1.590	934	9

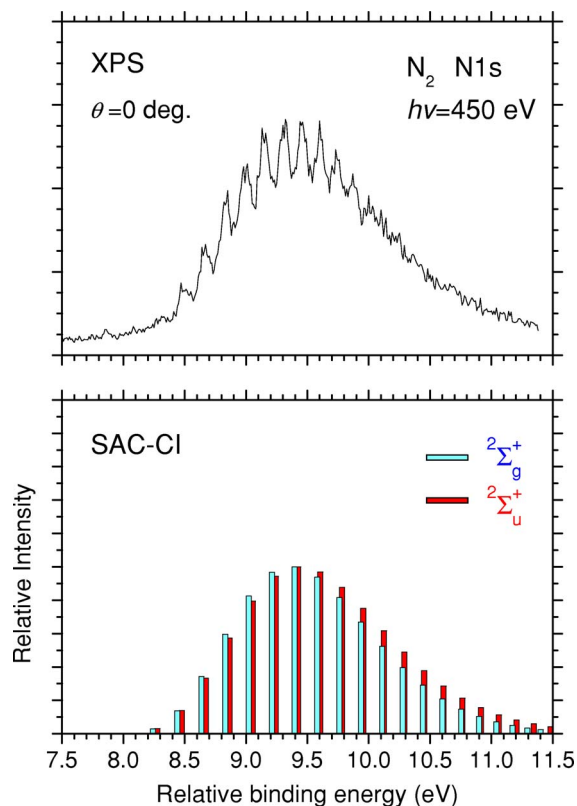


FIG. 5. Experimental and SAC-CI vibrationaly resolved spectra of the N 1s satellite bands of Σ symmetry. Experimental spectrum is recorded at incident photon energy of 450 eV.

calculated g - u splitting for these satellites is ~ 40 meV, much smaller than that of the single-hole state of 101 meV. The geometry relaxation for the ${}^2\Pi_{g,u}$ states is much smaller than for the ${}^2\Sigma_{g,u}^+$ states, as is the case for CO: the equilib-

rium distances of the lower and higher ${}^2\Pi_g$ states are $r_e = 1.161$ and 1.186 Å. The geometry change of these states, 0.066 and 0.091 Å, is larger than the corresponding changes for CO, 0.042 and 0.068 Å.¹¹ This is because the ${}^2\Pi_{g,u}$ states of N_2 have the character of $\sigma - \pi^*$ transitions and the ${}^2\Pi$ states of CO are $n - \pi^*$ transitions. The g - u splitting for these states was calculated to be very small as ~ 10 and ~ 20 meV for lower and higher ${}^2\Pi_{g,u}$ states, respectively. The potential energy curves of two pairs of the ${}^2\Delta_{g,u}$ and ${}^2\Sigma_{g,u}^-$ states are almost parallel to those of the ${}^2\Sigma_{g,u}^+$ states. The lower ${}^2\Delta_{g,u}$ and ${}^2\Sigma_{g,u}^-$ states nearly degenerate and their equilibrium distances are 1.288 Å for the ${}^2\Delta_g$ and ${}^2\Sigma_g^-$ states. The reason for the similarity of the ${}^2\Sigma_g^+$, ${}^2\Delta_g$, and ${}^2\Sigma_g^-$ can be found in the fact that all these states have the same $1\sigma_u^{-1}1\pi_u^{-1}1\pi_g^1$ configuration.

For simulating the vibrationally resolved photoelectron spectrum, vibrational wave functions and FC factors were obtained by a numerical grid method. The SAC-CI theoretical spectra thus obtained for the ${}^2\Sigma_g^+$ and ${}^2\Sigma_u^+$ states are compared with the experimental photoelectron satellite spectra recorded at 450 eV in Fig. 5. The calculated FC factors are summarized in Table III. The theoretical spectra were shifted in energy by $+0.11$ eV for both ${}^2\Sigma_{g,u}^+$ states; the calculated binding energy was scaled relative to the averaged values of g and u mainlines. The theoretical spectrum for ${}^2\Sigma_{g,u}^+$ has a maximum intensity at $v' = 6$, reproducing the shape of the experimental spectrum. The activation of the high vibrational states is due to the large geometry relaxation, i.e., the elongation of the bond length by 0.164 Å. Deviations between the theoretical and experimental spectra in the higher vibrational states can be attributed to the errors of the calculated potential curves for large nuclear distances.

Figure 6 compares the SAC-CI spectra for the ${}^2\Pi_{g,u}$

TABLE III. Vibrational levels (ΔE , in eV) and relative Franck-Condon factors (FCFs) of the satellite states calculated by the SAC-CI method.

No.	${}^2\Sigma_u^+$		${}^2\Sigma_g^+$		${}^2\Pi_u$ (lower)		${}^2\Pi_g$ (lower)		${}^2\Pi_u$ (higher)		${}^2\Pi_g$ (higher)	
	ΔE	FCF	ΔE	FCF	ΔE	FCF	ΔE	FCF	ΔE	FCF	ΔE	FCF
0	0.000	0.031	0.000	0.029	0.000	1.000	0.000	0.994	0.000	0.620	0.000	0.567
1	0.199	0.139	0.198	0.138	0.218	0.880	0.227	1.000	0.247	1.000	0.253	0.985
2	0.395	0.333	0.394	0.342	0.434	0.432	0.448	0.575	0.488	0.953	0.499	1.000
3	0.588	0.574	0.587	0.597	0.646	0.159	0.665	0.252	0.722	0.705	0.739	0.781
4	0.778	0.795	0.779	0.826	0.855	0.050	0.877	0.094	0.951	0.449	0.972	0.520
5	0.965	0.944	0.968	0.968	1.061	0.014	1.084	0.032	1.174	0.258	1.199	0.312
6	1.148	1.000	1.154	1.000					1.391	0.139	1.420	0.173
7	1.328	0.970	1.337	0.938					1.604	0.070	1.635	0.091
8	1.505	0.878	1.517	0.816					1.811	0.034	1.845	0.046
9	1.678	0.752	1.694	0.669					2.015	0.016	2.050	0.022
10	1.847	0.618	1.866	0.524								
11	2.013	0.490	2.035	0.396								
12	2.175	0.379	2.199	0.291								
13	2.332	0.287	2.358	0.209								
14	2.486	0.213	2.511	0.148								
15	2.637	0.157	2.658	0.104								
16	2.783	0.114	2.798	0.072								
17	2.927	0.083	2.929	0.050								
18	3.068	0.060	3.049	0.034								

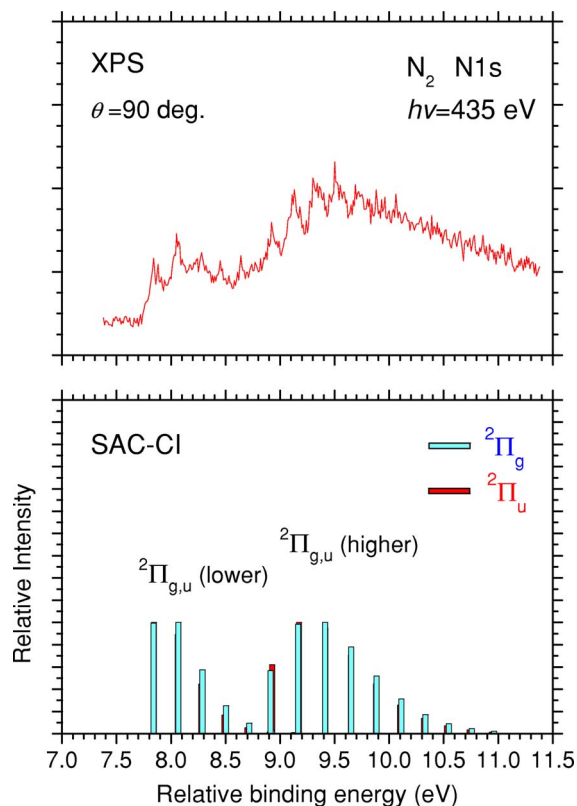


FIG. 6. Experimental and SAC-CI vibrational spectra of the N 1s satellite bands of Π symmetry. Experimental spectrum is recorded at incident photon energy of 435 eV.

states with the experimental photoelectron satellite spectra recorded at 435 eV, where the 90° spectrum dominantly represents the Π component. The theoretical spectra were shifted in energy by -0.49 and -0.33 eV for the lower and higher ${}^2\Pi_{g,u}$ states, with the same shifts for both gerade and ungerade states. The relative intensities of the bands were adjusted so that the theoretical spectra gave overall agreement with the experimental spectra: the vibrational intensity ratios were determined by the FC factors. For the lower ${}^2\Pi_g$ band, the vibrational levels of $v'=0$ and $v'=1$ have almost the same intensity and the higher levels are populated in the gerade state. In the higher Π band, $v'=2$ has the maximum intensity. Since the ${}^2\Pi_g$ state has a hole in the $1\sigma_g$ orbital, the geometry relaxation of the ${}^2\Pi_g$ state is larger than that of the ${}^2\Pi_u$ state and the theoretical spectra reflect this difference of geometry change. The higher vibrational levels are more strongly populated than for CO, since the satellites of N₂ are populated by $\sigma-\pi^*$ transitions, as noted above. The theoretical spectra for the ${}^2\Delta_{g,u}$ and ${}^2\Sigma_{g,u}^-$ symmetries appear at higher energies, peaking at ~ 10.0 eV (lower ${}^2\Delta_{g,u}$ and ${}^2\Sigma_{g,u}^-$), ~ 11.0 eV (higher ${}^2\Delta_{g,u}$), and ~ 11.4 eV (higher ${}^2\Sigma_{g,u}^-$). These states are located just above the present vibrational band and can be assigned to the band (b1–b3) observed by Kempgens *et al.*¹⁷ The present experimental spectra also show a continuous shape in this region. The higher ${}^2\Sigma_{g,u}^+$ states (singlet satellites) are repulsive in the FC region and have shallow minimum at about 1.57 – 1.59 Å; no vibrational structure is expected for these states.

V. CONCLUSION

We have observed vibrationally resolved N 1s photoelectron mainline and satellites of the gaseous N₂ molecule at high energy resolution. The spectroscopic constants were reported for the mainline $1\sigma_u$ and $1\sigma_g$ single-hole states, and the geometry relaxations of these mainline states were studied in the light of the FC ratios $I(v'=1)/I(v'=0)$ measured at the sudden limit. The angle-resolved spectra allow us to assign the observed satellite bands to one pair of ${}^2\Sigma^+$ states, $1\sigma_u^{-1}1\pi_u^{-1}1\pi_g^1({}^2\Sigma_g^+)$ and $1\sigma_g^{-1}1\pi_u^{-1}1\pi_g^1({}^2\Sigma_u^+)$, and two pairs of ${}^2\Pi$ states, $1\sigma_u^{-1}3\pi_g^{-1}1\pi_g^1({}^2\Pi_g)$ and $1\sigma_u^{-1}3\sigma_g^{-1}1\pi_g^1({}^2\Pi_u)$. Excellent agreement between observed and calculated vibrational spectra was obtained and the vibrational excitation of these bands was well interpreted by the theoretical calculations. The SAC-CI method calculated that the geometrical changes of ${}^2\Sigma_{g,u}^+$ states are as large as ~ 0.16 Å, while those of ${}^2\Pi$ are small as 0.07 – 0.09 Å. The method also predicted a difference of the geometry change between the gerade and ungerade shake-up states as 0.000 – 0.004 Å. The g - u splitting of these shake-up states was calculated to be about 10 – 40 meV, which is smaller than that of the main line ~ 100 meV. The vibrationally resolved spectra and geometry relaxation of these satellites were discussed in detail by comparing them with those of CO.

ACKNOWLEDGMENTS

The experiment was carried out with the approval of the SPring-8 program review committee. This study was supported by a Grant for Creative Scientific Research from the Ministry of Education, Science, Culture, and Sports of Japan and by Grants-in-Aid for Scientific Research from the Japanese Society for the Promotion of Science.

- ¹G. Herzberg, *Molecular Spectra and Molecular Structure I. Spectra of Diatomic Molecules* (Van Nostrand, London, 1967).
- ²K. Ueda, J. Phys. B **36**, R1 (2003).
- ³U. Hergenhahn, J. Phys. B **37**, R89 (2004).
- ⁴K. J. Borge, L. J. Saethre, T. D. Thomas, T. X. Carroll, N. Berrah, J. D. Bozek, and E. Kukk, Phys. Rev. A **63**, 012506 (2001).
- ⁵T. Karlsen, L. J. Saethre, K. J. Borge, N. Berrah, J. D. Bozek, T. X. Carroll, and T. D. Thomas, J. Phys. Chem. A **105**, 7700 (2001).
- ⁶M. Matsumoto, K. Ueda, E. Kukk *et al.*, Chem. Phys. Lett. **417**, 89 (2006).
- ⁷H. Nakatsuji, Chem. Phys. Lett. **59**, 362 (1978).
- ⁸H. Nakatsuji, Chem. Phys. Lett. **67**, 329 (1979).
- ⁹H. Nakatsuji, Chem. Phys. Lett. **177**, 331 (1991).
- ¹⁰H. Nakatsuji, *Computational Chemistry, Review of Current Trends* (World Scientific, Singapore, 1997).
- ¹¹K. Ueda, M. Hoshino, T. Tanaka *et al.*, Phys. Rev. Lett. **94**, 243004 (2005).
- ¹²U. Hergenhahn, O. Kugeler, A. Rüdell, E. E. Rennie, and A. M. Bradshaw, J. Phys. Chem. A **105**, 5704 (2001).
- ¹³A. Thiel, J. Schirmer, and H. Köppel, J. Chem. Phys. **119**, 2088 (2003).
- ¹⁴G. Angonoa, I. Walter, and J. Schirmer, J. Chem. Phys. **87**, 6789 (1987).
- ¹⁵U. Gelius, J. Electron Spectrosc. Relat. Phenom. **5**, 985 (1974).
- ¹⁶S. Svensson, A. Naves de Brito, M. P. Kaene, N. Correia, L. Karlsson, C.-M. Liegener, and H. Ågren, J. Phys. B **25**, 135 (1992).
- ¹⁷B. Kempgens, A. Kivimäki, M. Neeb, H. M. Köppe, A. M. Bradshaw, and J. Feldhaus, J. Phys. B **29**, 5389 (1996).
- ¹⁸M. Ehara, J. Heseegawa, and H. Nakatsuji, in *Theory and Applications of Computational Chemistry: The First 40 Years, A Volume of Technical and Historical Perspectives* (Elsevier, New York, 2005).
- ¹⁹R. Sankari, M. Ehara, H. Nakatsuji, Y. Senba, K. Hosokawa, H. Yoshida, A. D. Fanis, Y. Tamenori, S. Aksela, and K. Ueda, Chem. Phys. Lett. **380**, 647 (2003).

- ²⁰K. Kuramoto, M. Ehara, and H. Nakatsuji, *J. Chem. Phys.* **122**, 014304 (2005).
- ²¹K. Kuramoto, M. Ehara, H. Nakatsuji, M. Kitajima, H. Tanaka, A. D. Fanis, Y. Tamenori, and K. Ueda, *J. Electron Spectrosc. Relat. Phenom.* **142**, 253 (2005).
- ²²H. Ohashi, E. Ishiguro, Y. Tamenori, H. Kishimoto, M. Tanaka, M. Irie, and T. Ishikawa, *Nucl. Instrum. Methods Phys. Res. A* **467–468**, 529 (2001).
- ²³H. Ohashi, E. Ishiguro, Y. Tamenori *et al.*, *Nucl. Instrum. Methods Phys. Res. A* **467–468**, 533 (2001).
- ²⁴T. Tanaka and H. Kitamura, *J. Synchrotron Radiat.* **3**, 47 (1996).
- ²⁵Y. Shimizu, H. Ohashi, Y. Tamenori *et al.*, *J. Electron Spectrosc. Relat. Phenom.* **114–116**, 63 (2001).
- ²⁶P. S. Bagus and H. F. Schaefer III, *J. Chem. Phys.* **56**, 224 (1972).
- ²⁷G. A. Sawatzky and A. Lenselink, *J. Chem. Phys.* **72**, 3748 (1980).
- ²⁸A. Schaefer, C. Huber, and R. Ahlrichs, *J. Chem. Phys.* **100**, 5829 (1994).
- ²⁹T. H. Dunning, Jr., *J. Chem. Phys.* **90**, 1007 (1989).
- ³⁰H. Nakatsuji, *J. Chem. Phys.* **83**, 713 (1985).
- ³¹M. Ehara and H. Nakatsuji, *Chem. Phys. Lett.* **282**, 347 (1998).
- ³²M. Ehara, M. Ishida, K. Toyota, and H. Nakatsuji, in *Reviews in Modern Quantum Chemistry* (World Scientific, Singapore, 2002).
- ³³H. Nakatsuji, *Chem. Phys.* **75**, 425 (1983).
- ³⁴M. J. Frisch *et al.*, GAUSSIAN 03, Gaussian Inc., Pittsburgh, PA, 2003.
- ³⁵M. Alagia, R. Richter, S. Stranges *et al.*, *Phys. Rev. A* **71**, 012506 (2005).
- ³⁶G. A. Worth, M. H. Beck, A. Jackle, and H.-D. Meyer, The MCTDH Package, version 8.3, University Heidelberg, Heidelberg, Germany, 2003.
- ³⁷L. S. Cederbaum, W. Domcke, J. Schirmer, and W. V. Niessen, *Adv. Chem. Phys.* **65**, 115 (1986).
- ³⁸A. D. O. Bawagan and E. R. Davidson, *Adv. Chem. Phys.* **110**, 215 (1999).
- ³⁹U. Becker and D. A. Shirley, *Phys. Scr.*, T **T31**, 56 (1990).
- ⁴⁰L. Ungier and T. D. Thomas, *Phys. Rev. Lett.* **53**, 435 (1984).
- ⁴¹J. Schirmer, G. Braunstein, and V. McKoy, *Phys. Rev. A* **44**, 5762 (1991).